

AD 609039

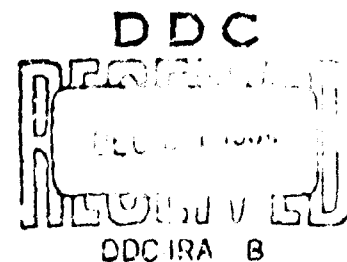
Cm 102-4



DEBRIS DISTRIBUTION
IN
UNDERWATER EXPLOSIONS

COPY	2	OF	3	32.10
*** COPY				\$.2.00
MICROFICHE				\$.6.50

ANNUAL SUMMARY REPORT
CONTRACT NO. NOnr 3095(00)
JANUARY 1964



Malaker
Laboratories, Inc.

Prepared for
DEPARTMENT OF THE NAVY
OFFICE OF NAVAL RESEARCH
WASHINGTON 25, D. C.

**Best
Available
Copy**

*DEBRIS DISTRIBUTION IN UNDERWATER
EXPLOSIONS*

*Prepared By
MALAKER LABORATORIES, INC.
High Bridge, N. J.*

*ANNUAL SUMMARY REPORT
CONTRACT NO. NOnr 3095(00)
JANUARY 1964*

*Prepared For

DEPARTMENT OF THE NAVY
OFFICE OF NAVAL RESEARCH
WASHINGTON 25, D. C.*

DEBRIS DISTRIBUTION IN UNDERWATER
EXPLOSIONS

Prepared by

EARL F. BRYANT

MALAKER LABORATORIES, INC.
High Bridge, N. J.

ANNUAL SUMMARY REPORT

CONTRACT NO. NOnr 3095(00)

JANUARY 1964

APPROVED BY

Dr. S. F. Malaker
Dr. S. F. Malaker

Prepared for

DEPARTMENT OF THE NAVY

OFFICE OF NAVAL RESEARCH

TABLE OF CONTENTS

	<i>Page</i>
<i>Introduction.....</i>	<i>1</i>
<i>Underwater Bubble Studies.....</i>	<i>2</i>
<i>Scaling.....</i>	<i>3</i>
<i>Bubble Study Results.....</i>	<i>5</i>
<i>Bubble Study Conclusions.....</i>	<i>6</i>
<i>Above Surface Study.....</i>	<i>6</i>
<i>Table I.....</i>	<i>9</i>
<i>List of Illustrations.....</i>	<i>10</i>

INTRODUCTION

Malaker Laboratories has been engaged in explosion simulation studies for the Office of Naval Research under Contract No. NOnr 3095(00) for three years. Previous reports issued include Numbers CM 102-1, CM 102-2 and CM 102-3.

During this reporting period (January 1, 1963, to January 1, 1964), above and below surface effects of underwater explosions have been investigated through use of exploding wire equipment. A correlation between bubble phases and deposition of debris has been sought and a means has been devised to measure debris concentration in certain water column areas. This report includes data obtained from underwater bubble studies and a description of the apparatus being prepared for the above surface investigation. Data from more than sixty underwater bubble experiments has been obtained. The results of shots not reported here are being reduced and will be submitted in a supplementary report along with data on above surface tests in progress at the time of this writing.

Underwater debris deposition was studied by means of high speed motion pictures of wires exploded in light mineral oil. Above surface effects of radioactive exploding wires submerged

in scintillation solution are being investigated by means of a sensitive photoelectric scanner.

UNDERWATER BUBBLE STUDIES

A 10 joule wire exploder was constructed and arranged to explode silver ribbon material in a beaker filled with light mineral oil (see Fig. 2). Mineral oil was used to eliminate the electrical losses associated with water. The low energy system was selected to minimize the problems of lighting and photography. The effects of gravity on bubble migration have been shown to be a function of hydrostatic pressure¹. Thus, if scale model experiments such as these are to produce significant prototype information, the surface pressure must be reduced below atmospheric. Experiments were conducted, therefore, under an evacuated bell jar. Strong backlighting was used and during the violent phases of the event a high speed motion analysis camera (Fairchild HS401) recorded the action. In many cases the movie camera was run until cessation of violence, to record character and position of the debris cloud. In other instances, a still camera was set up immediately after the shot to photograph this cloud. Fig. 2 is such a photograph obtained subsequent to

¹Cole, R. H., UNDERWATER EXPLOSIONS, Princeton University Press, 1948, pp. 291, 292.

the firing depicted in Fig. 1 (Fig. 1 and similar figures were prepared by enlarging individual frames selected from the 16 mm movie film--in general, selected frames show early bubble maxima and minima and enough later frames to establish migration direction). Figs. 1 through 9 present the results obtained from eight experiments.

SCALING

The results of the eight experiments reported here are compiled in Table I. Event violence is obviously a function of the physical size of the exploding wire and of the electrical energy actually converted in the event. Direct measurement of the energy is not practical. Therefore, recourse is made to measurement of the optical records and use of accepted hydrodynamical theory for derivation of the desired energy release. A reliable first approximation to the energy involved in producing a bubble (that is, total event yield less both shock wave and bubble internal energy) is given by:

$$Y = \frac{4\pi}{3} P_0 a_m^3 \quad 2$$

where Y = fraction of total yield involved in bubble expansion

P_0 = hydrostatic pressure

a_m = maximum bubble radius

²Op. Cit. Equation 8.6, p. 275

Measurements of maximum bubble radius listed in the table were scaled from high speed motion picture film. The vertical bubble dimension was selected as being the least distorted by refraction due to the cylindrical, oil-filled chamber. Partition of explosion energy between shock wave and gas sphere has been determined with some care by experimenters working with various chemical explosives. The shock wave fraction has been shown to be a definite attribute of the explosive chemical composition and physical form. Buntzen³ has investigated the energy partition with underwater exploding wires and concludes that 31.0% of explosion yield is involved in bubble formation. No transient pressure measurements were made in the series reported here so that independent determination of partition values is not possible. Therefore, the 31% figure will be used as an acceptable estimate. Total yield figures listed in the table are not unreasonable since 9.1 joules was stored in the capacitor for each shot (10 microfarads at 1350 volts).

The oscillation period of bubbles formed by chemical explosives is given by:

$$T = k \frac{Y^{1/3}}{P^{5/6}}$$

4

³R. R. Buntzen, "The Use of Exploding Wires in The Study of Small-Scale Explosions," Hydra Program, Technical Memorandum No. 133, March, 1962.

⁴Op. Cit., P. 280, Equation 8.11

where T is bubble oscillation period

k is a coefficient determined
by the explosive

Y is the energy available for
bubble formation

P is the hydrostatic pressure

No value for k is known for the underwater exploding wire.

Therefore, the equation is solved for k :

$$k = \frac{T P^{5/6}}{Y^{1/3}}$$

And values are found for each of the reported cases (see table column headed "Period Expression Coefficient k "). The resulting figures are far from constant so a graph relating the values of k with bubble energies was prepared. A linear relationship between k and Y is revealed by this graph. This definite departure from chemical explosion behavior is reported as a matter of interest but without attempt at explanation at this time.

BUBBLE STUDY RESULTS

Figs. 1 through 9 are photographs of the principal apparent explosion features for eight experiments. For instance, Fig. 1 shows the bubble phases obtained from motion pictures of one shot while Fig. 2 is a still photograph of the resulting debris cloud. The still photograph is omitted in subsequent figures but

considerable debris disposition can be detected in later movie frames. Several bubble migration directions occur and, in fact, these particular experiments were selected from over sixty shots for this preliminary report on the basis of the variety of migration directions.

BUBBLE STUDY CONCLUSIONS

It is quite apparent from every film record obtained to date that little or no metallic debris is deposited in the medium during early bubble oscillations. Further, it is clear that the debris is transported by the bubble and released in a relatively well defined cloud upon cessation of oscillation. The conclusion is fortified by the complete lack of debris cloud observed in Fig. 8 which depicts a bubble venting before cessation of oscillations.

The functional relation found between total yield and the period formula coefficient should make accurate scaling of the bubble behavior resulting from any type explosive device possible with the exploding wire equipment used in this study.

ABOVE SURFACE STUDY

No actual data has been obtained to date in this phase. The equipment has been fabricated and some initial calibrations

performed. This work will continue and be reported fully in the supplementary report.

Figs. 11 and 13 are photographs of the equipment to be used in this phase. Very small radioactive gold wires are exploded in a small open vessel placed inside the large evacuated steel chamber. The fluid medium is xylene solution of diphenyloxazole which produces scintillations in the presence of radioactive material. Four small objective lenses focus images of the explosion scene on related photomultiplier tubes and an interposed scanning disc breaks the image down into a sequential scan pattern by means of the spiral hole patterns visible in Fig. 13. A synchronous motor turns this scanning disc through a long belt to minimize the effects of the motor field on the sensitive photomultiplier tubes. A small incandescent lamp is used to illuminate a silicon solar cell through the hole pattern thus providing a disc position reference signal. "Video" signals from the photomultiplier tubes and the disc position reference signal are displayed on a dual beam oscilloscope through use of a 4-trace preamplifier. Fig. 12 is a photograph of two calibration tests performed on one scanning channel. In the upper oscilloscope view the top trace displays the photomultiplier output obtained with the bottom hole of the "calibration

scene" illuminated. In the lower oscilloscope view the upper trace was obtained with the next to bottom calibration scene aperture illuminated. In both oscilloscope photos the lower trace was produced by the reference lamp. Horizontal sweep rate was 50 milliseconds per centimeter.

TABLE I

<u>Shot</u>	<u>Ref. Fig.</u>	<u>Surface Pressure In. Hg.</u>	<u>Hydrostatic Pressure psi</u>	<u>Max. Bubble Radius in.</u>	<u>Derived Bubble Energy Joules</u>	<u>Observed Oscillation Period Seconds</u>	<u>Period Expression Coefficient κ</u>	<u>Total Explosion Yield $\phi_{31\%}$ to Bubble Joules</u>
8	1 2	6	3.14	0.88	1.01	.009	0.92	2.3
R5S1	3	2	1.16	0.99	0.54	.018	0.87	1.7
R6S1	4	0.5	0.44	1.2	0.36	.017	0.37	1.2
R7S1	5	0	0.203	1.7	0.47	.033	0.41	1.5
R9S1	6	0.3	0.35	2.1	1.55	.082	1.2	5.0
R10S2	7	10	5.1	0.86	1.6	.0045	0.39	5.2
R13S1	8	0	0.203	2.3	2.1	.163	1.4	6.8
R13S2	9	2	1.18	1.2	0.97	.021	0.96	3.1

LIST OF ILLUSTRATIONS

Fig.

- | | |
|-------------------|---|
| 1 and
3 thru 9 | <i>Explosion Sequences</i> |
| 2 | <i>Explosion Residue Following Sequence Shown in Fig. 1</i> |
| 10 | <i>Period Coefficient vs Total Yield</i> |
| 11 | <i>General View, Scintillation Scanner Equipment</i> |
| 12 | <i>Scanner Calibration Results</i> |
| 13 | <i>Scanner Disc</i> |

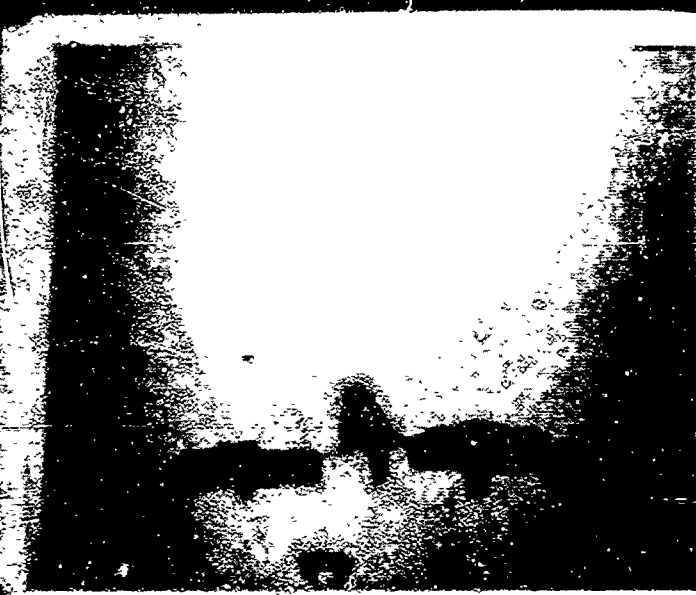
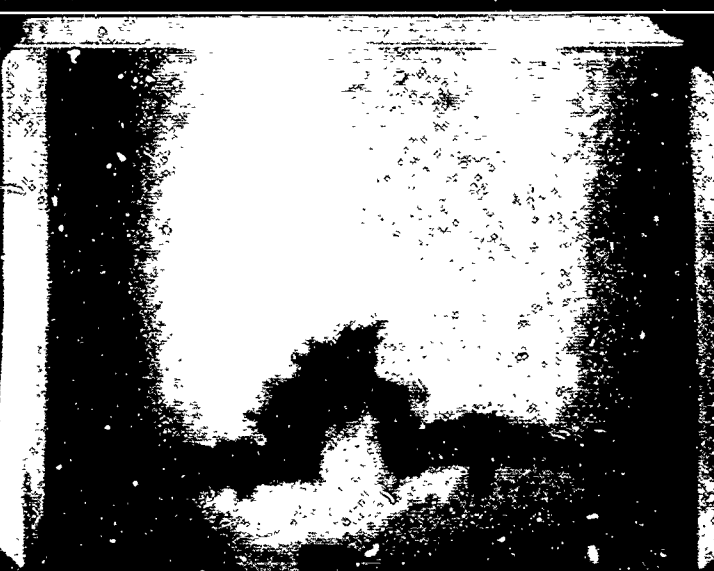
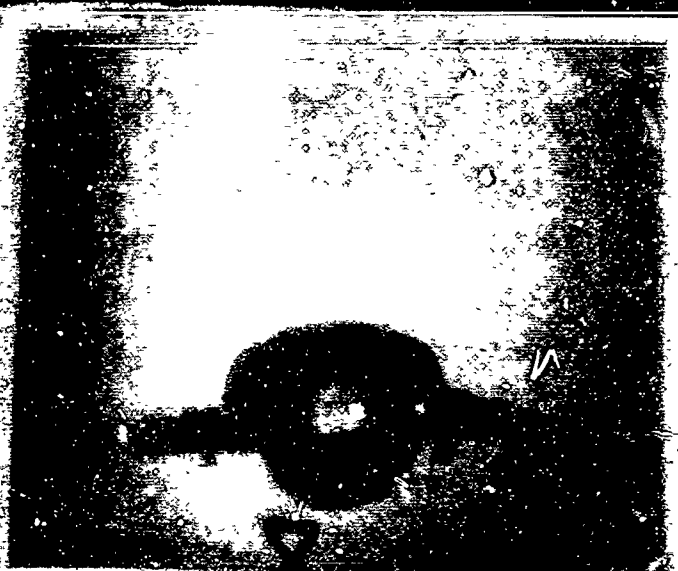
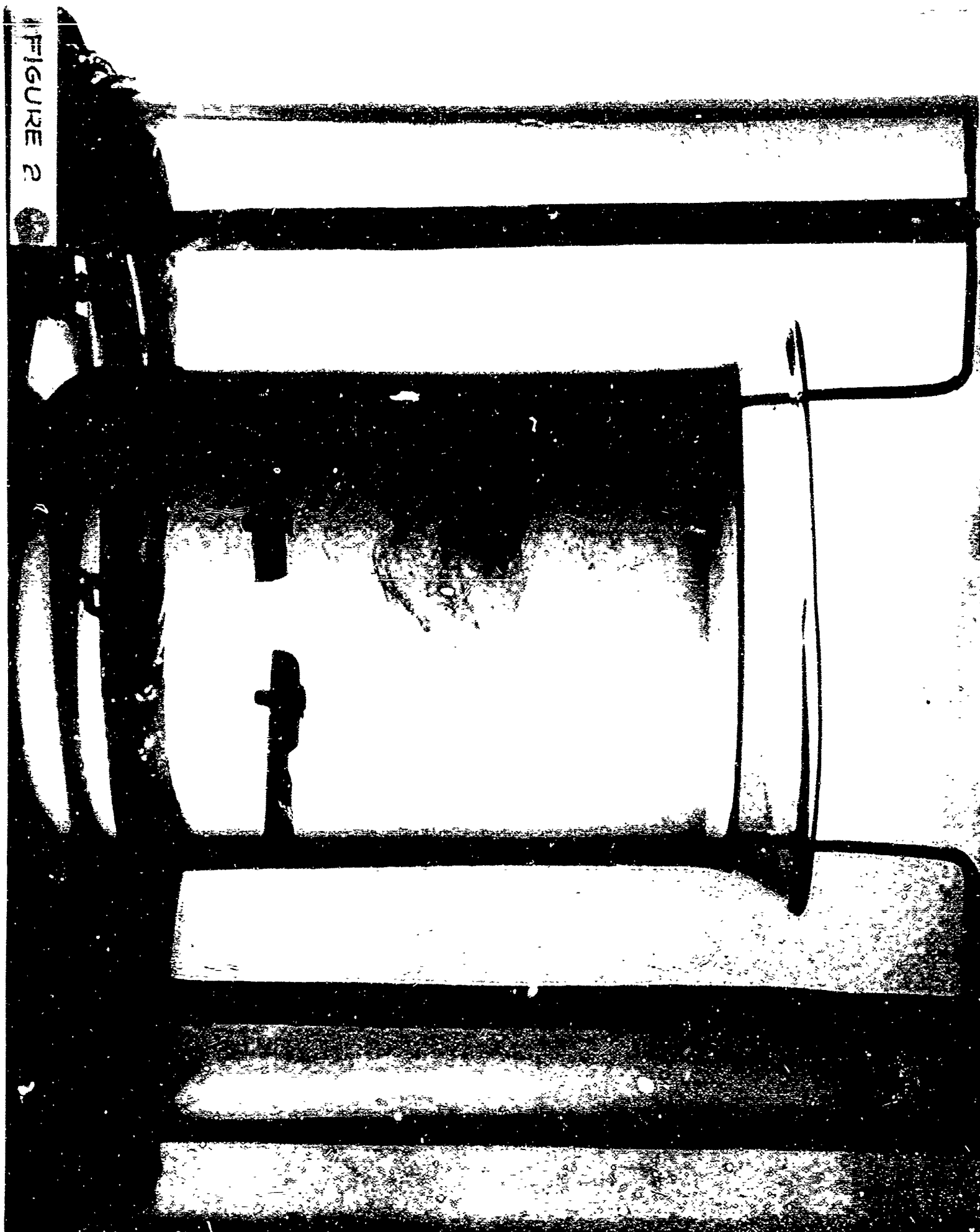
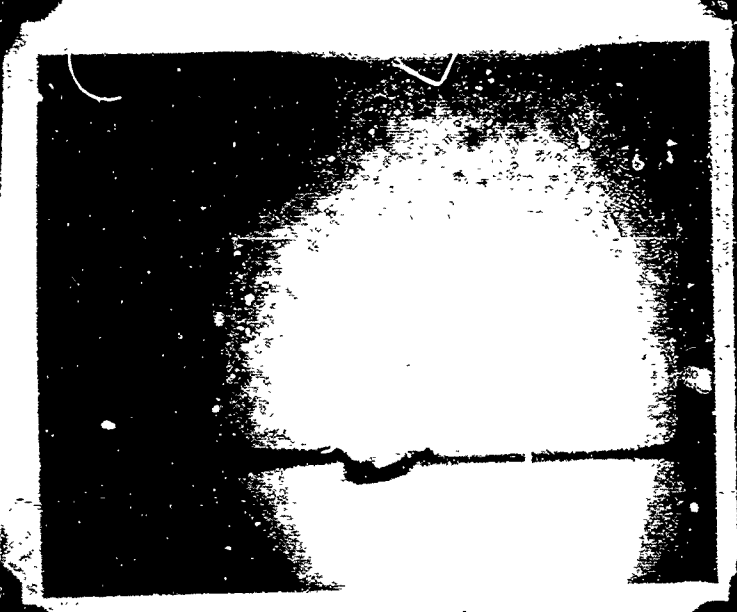
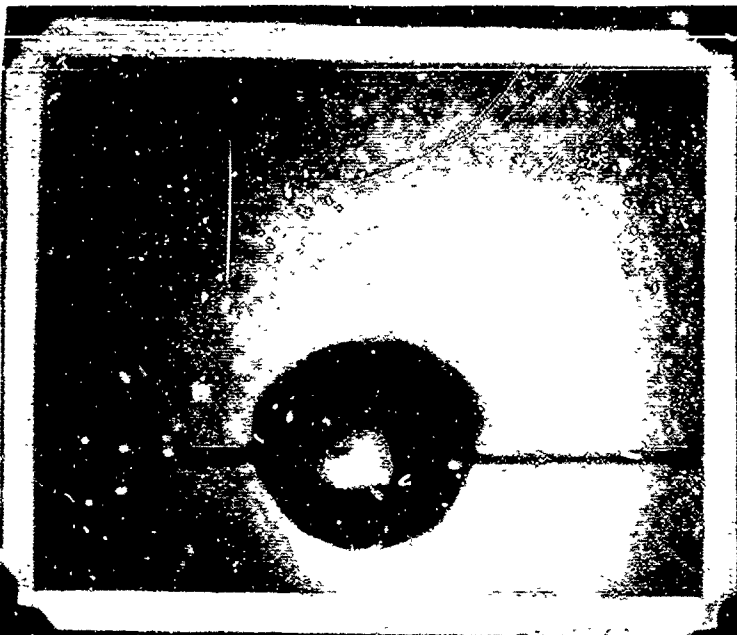


FIGURE 1

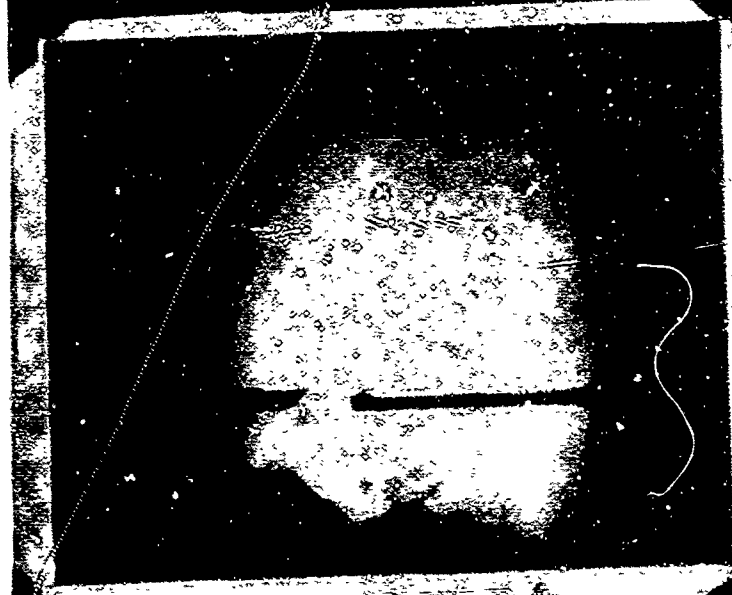
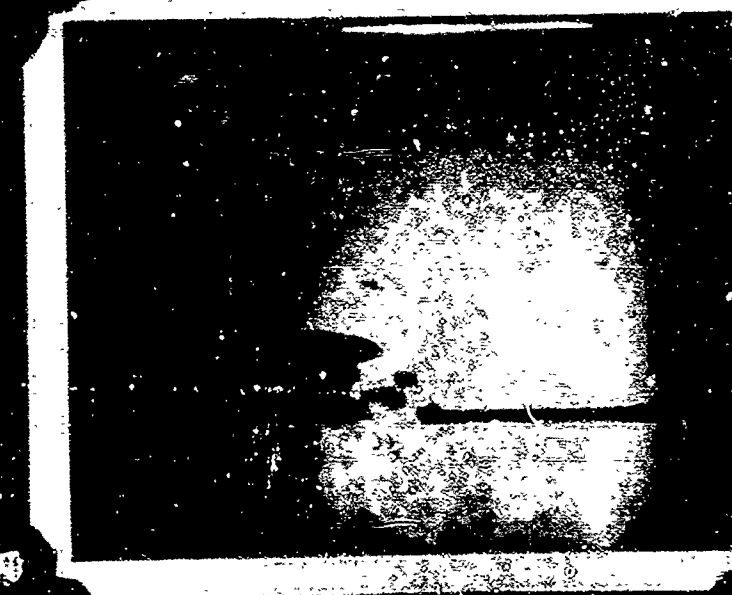
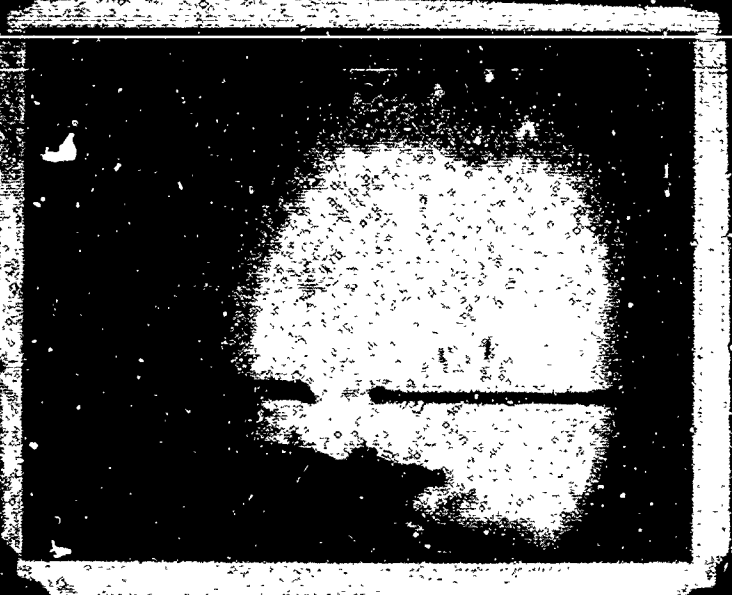
MEASUREMENTS: 6" dia.	
DEPTH: 6" dia.	
UPPER LEFT	FLAT MAX.
CENTER LEFT	FLAT MIN.
LOWER LEFT	FLAT MAX.
UPPER RIGHT	FLAT MIN.
LOWER RIGHT	FLAT MAX.

FIGURE 2





1. 1st
 2. 2nd
 3. 3rd
 4. 4th
 5. 5th
 6. 6th
 7. 7th
 8. 8th
 9. 9th
 10. 10th
 11. 11th
 12. 12th
 13. 13th
 14. 14th
 15. 15th
 16. 16th
 17. 17th
 18. 18th
 19. 19th
 20. 20th
 21. 21st
 22. 22nd
 23. 23rd
 24. 24th
 25. 25th
 26. 26th
 27. 27th
 28. 28th
 29. 29th
 30. 30th
 31. 31st
 32. 32nd
 33. 33rd
 34. 34th
 35. 35th
 36. 36th
 37. 37th
 38. 38th
 39. 39th
 40. 40th
 41. 41st
 42. 42nd
 43. 43rd
 44. 44th
 45. 45th
 46. 46th
 47. 47th
 48. 48th
 49. 49th
 50. 50th
 51. 51st
 52. 52nd
 53. 53rd
 54. 54th
 55. 55th
 56. 56th
 57. 57th
 58. 58th
 59. 59th
 60. 60th
 61. 61st
 62. 62nd
 63. 63rd
 64. 64th
 65. 65th
 66. 66th
 67. 67th
 68. 68th
 69. 69th
 70. 70th
 71. 71st
 72. 72nd
 73. 73rd
 74. 74th
 75. 75th
 76. 76th
 77. 77th
 78. 78th
 79. 79th
 80. 80th
 81. 81st
 82. 82nd
 83. 83rd
 84. 84th
 85. 85th
 86. 86th
 87. 87th
 88. 88th
 89. 89th
 90. 90th
 91. 91st
 92. 92nd
 93. 93rd
 94. 94th
 95. 95th
 96. 96th
 97. 97th
 98. 98th
 99. 99th
 100. 100th



PLATES 57
CONTENTS OF PLATES 57 - 60
- PRIVATE AND RETURN
- ALL PLATES

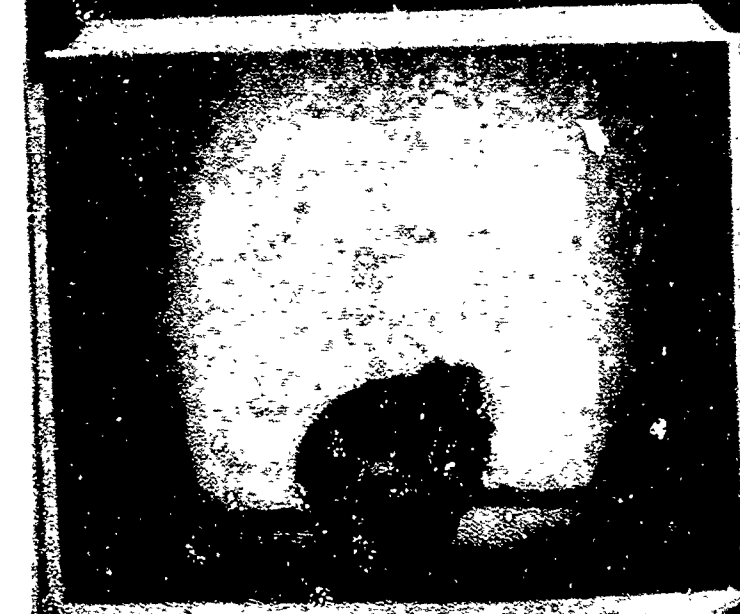
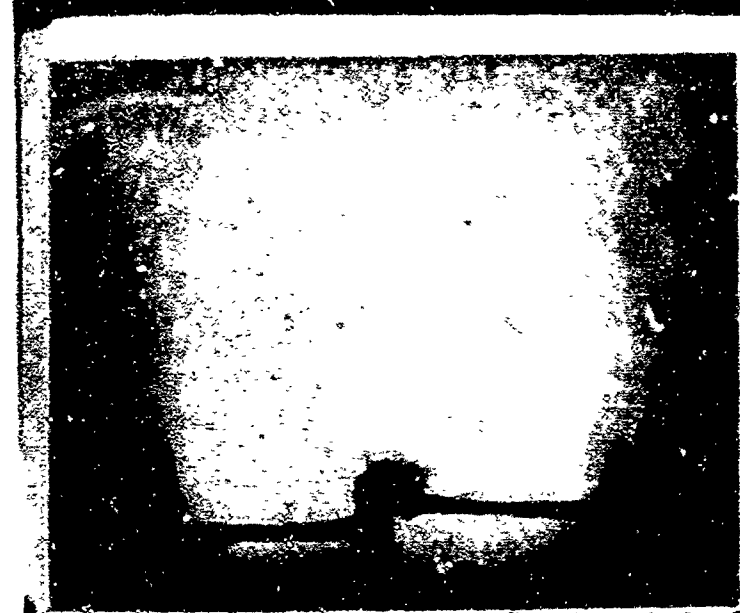
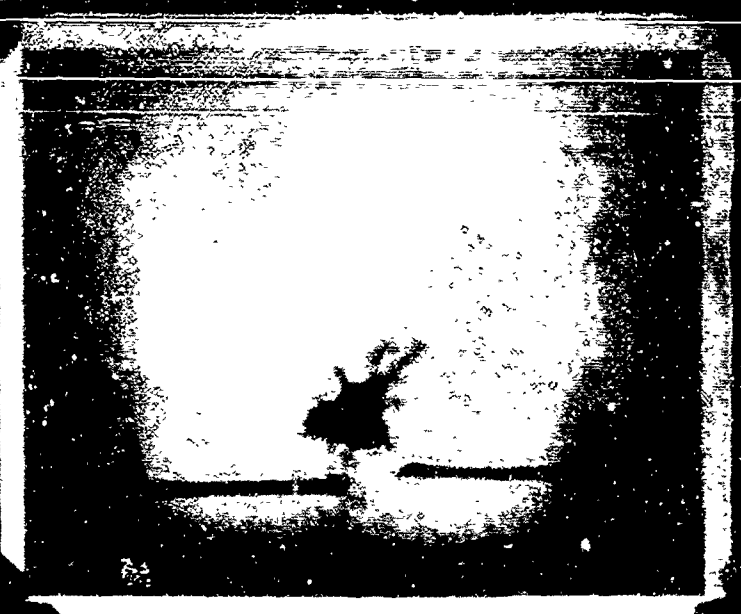


PHOTO 41
 SURFACE PRESSURE 0.5" Hg.
 DEPTH 17, 3" near surface
 UPPER LEFT FIRST AIR
 LOWER LEFT SECOND AIR
 UPPER RIGHT THIRD AIR
 LOWER RIGHT FOURTH AIR

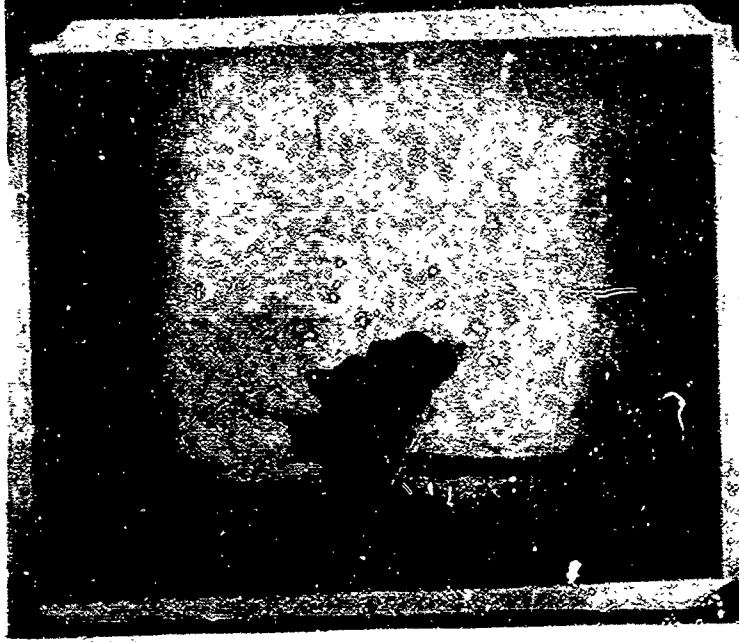
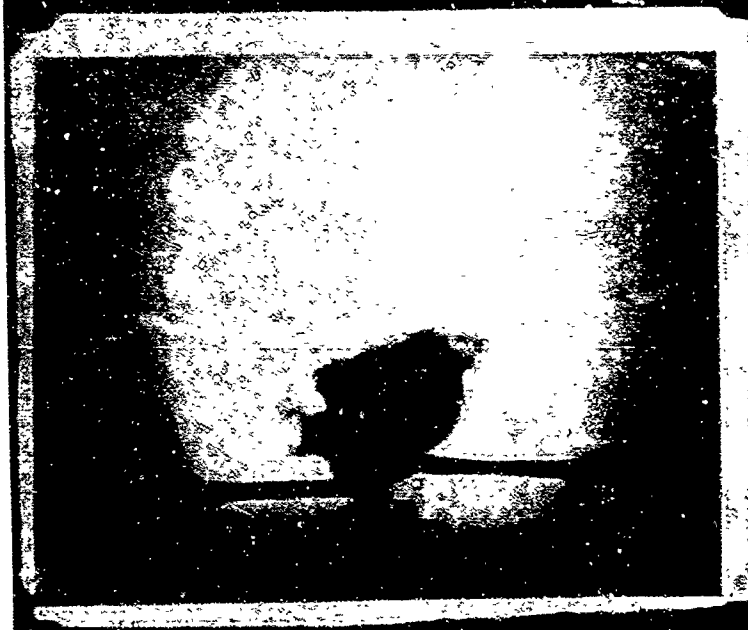
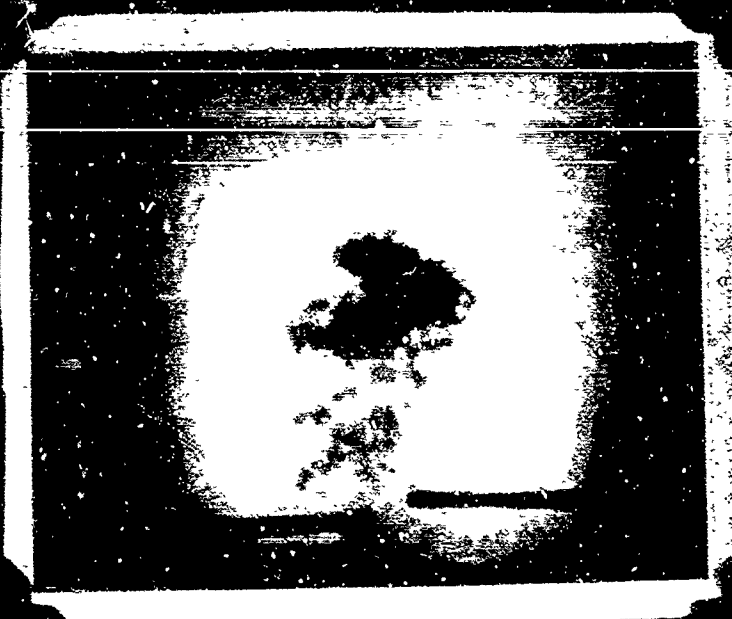
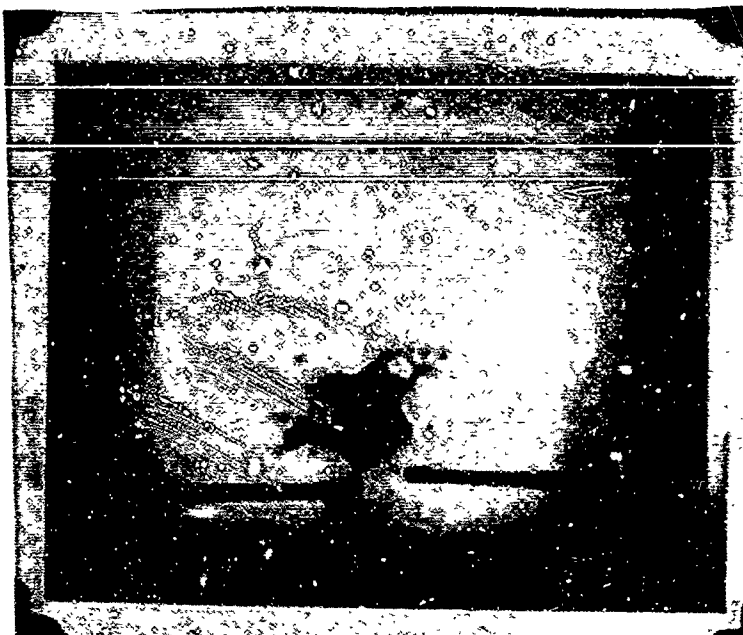


FIGURE 12
 CONTINUATION OF SEQUENCE 4A - RUBBER
 SLIPES WITH DEPLETING OSCILLATION

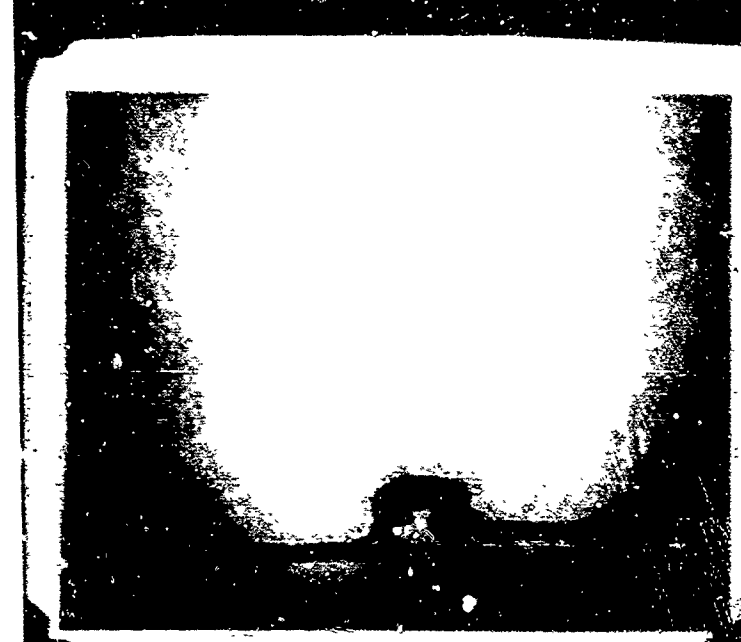
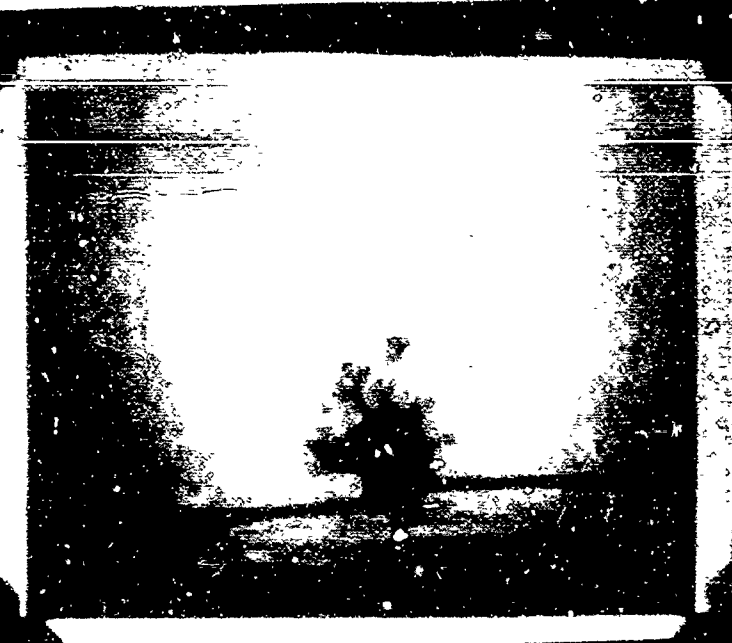
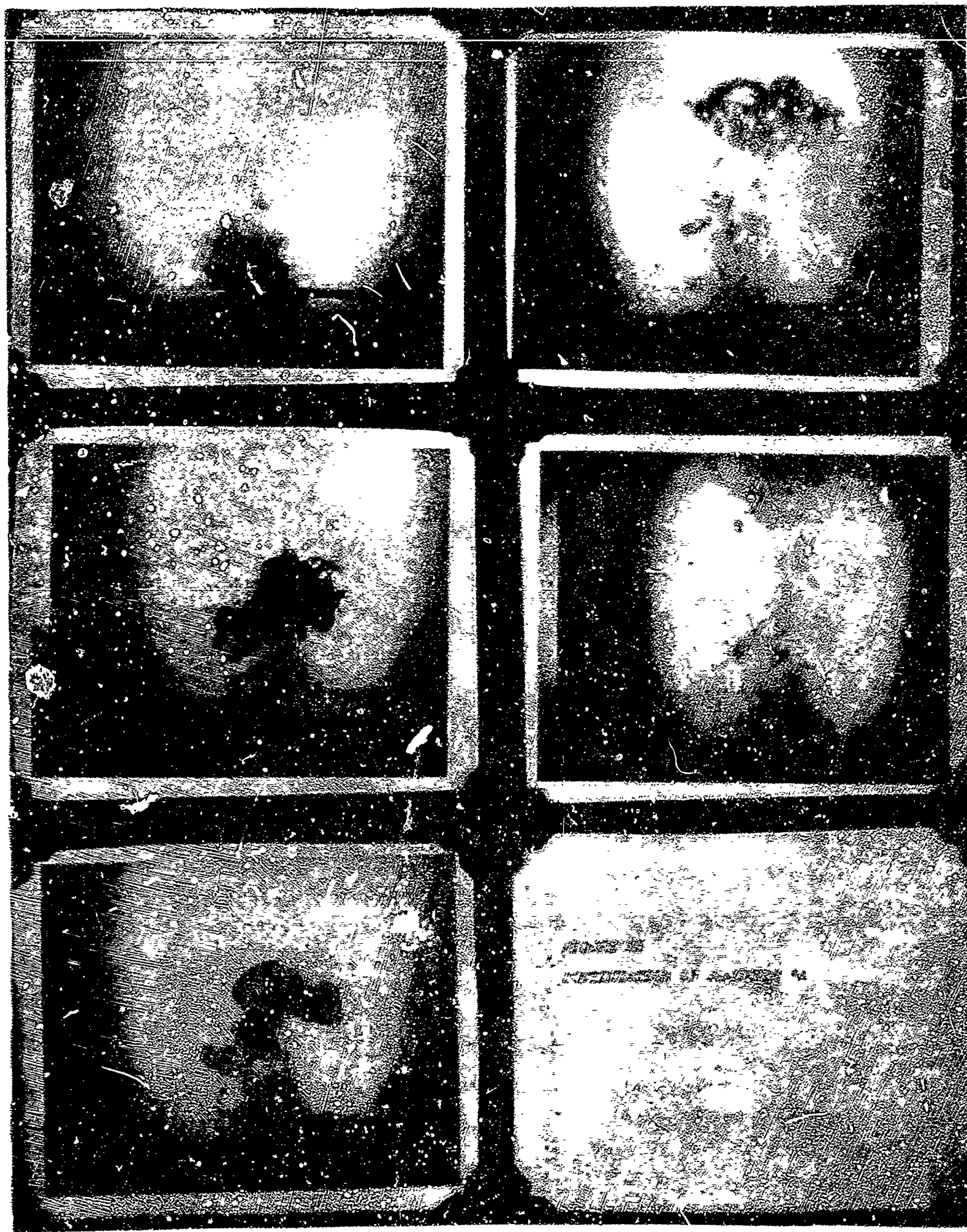
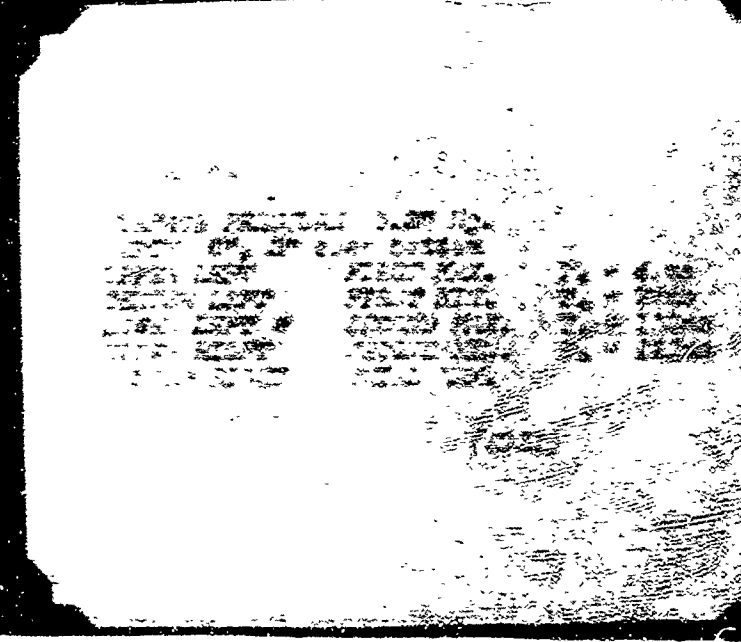
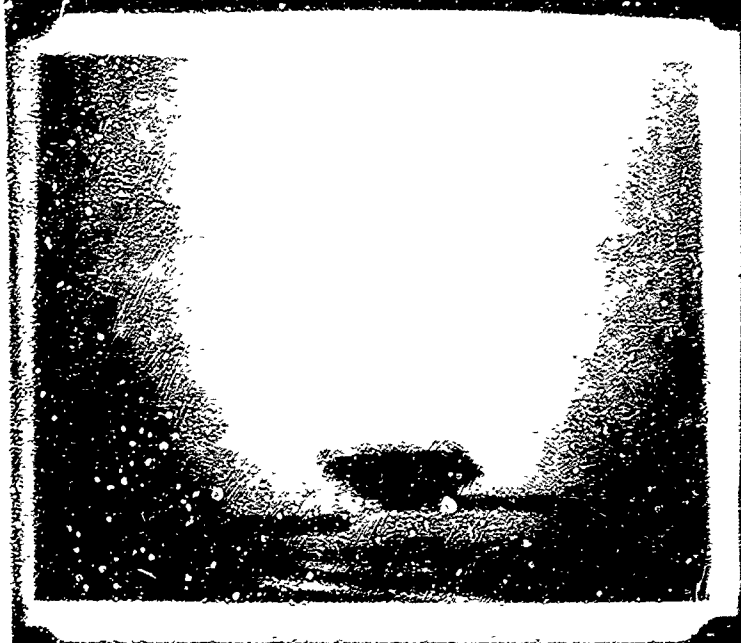


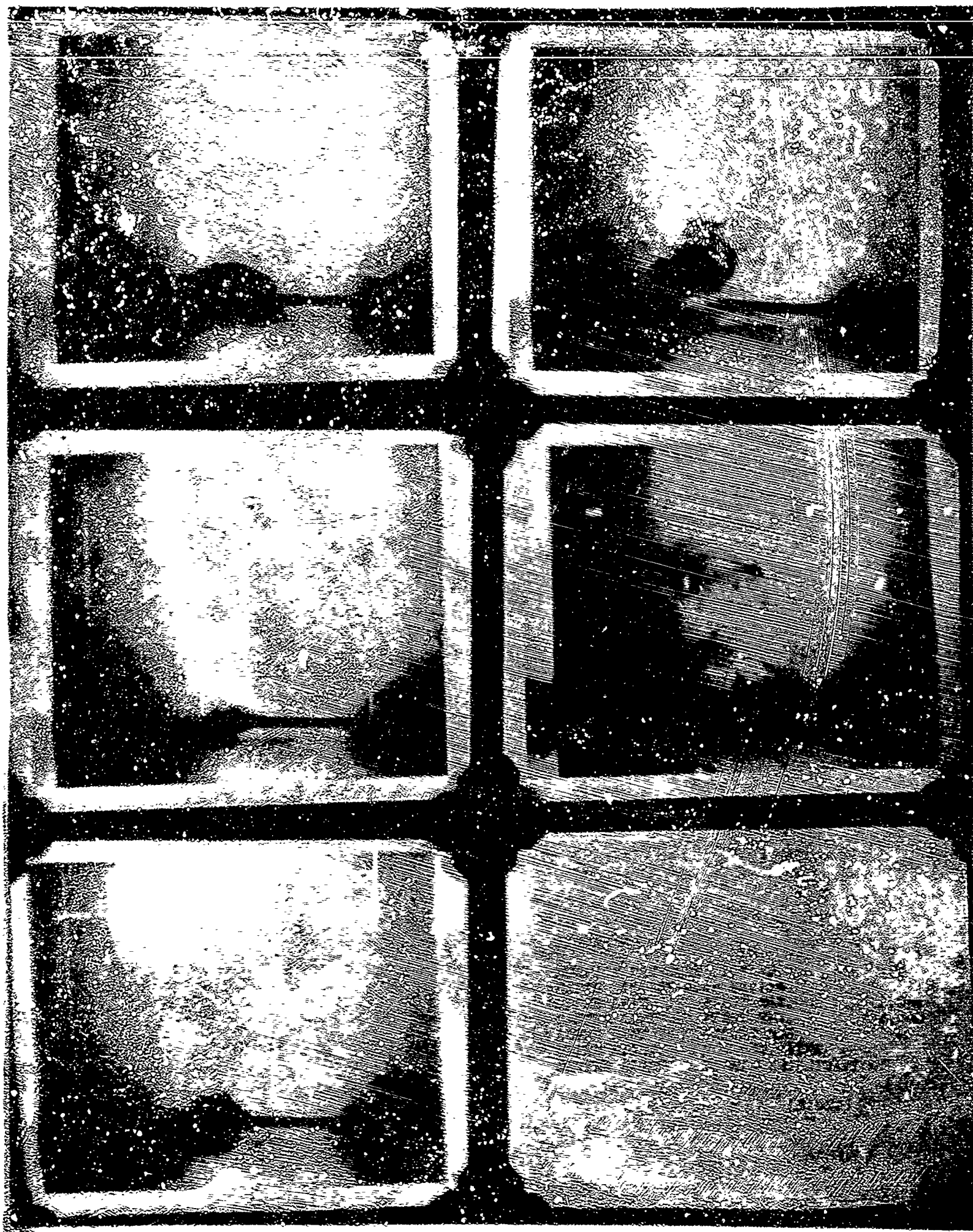
FIGURE 21

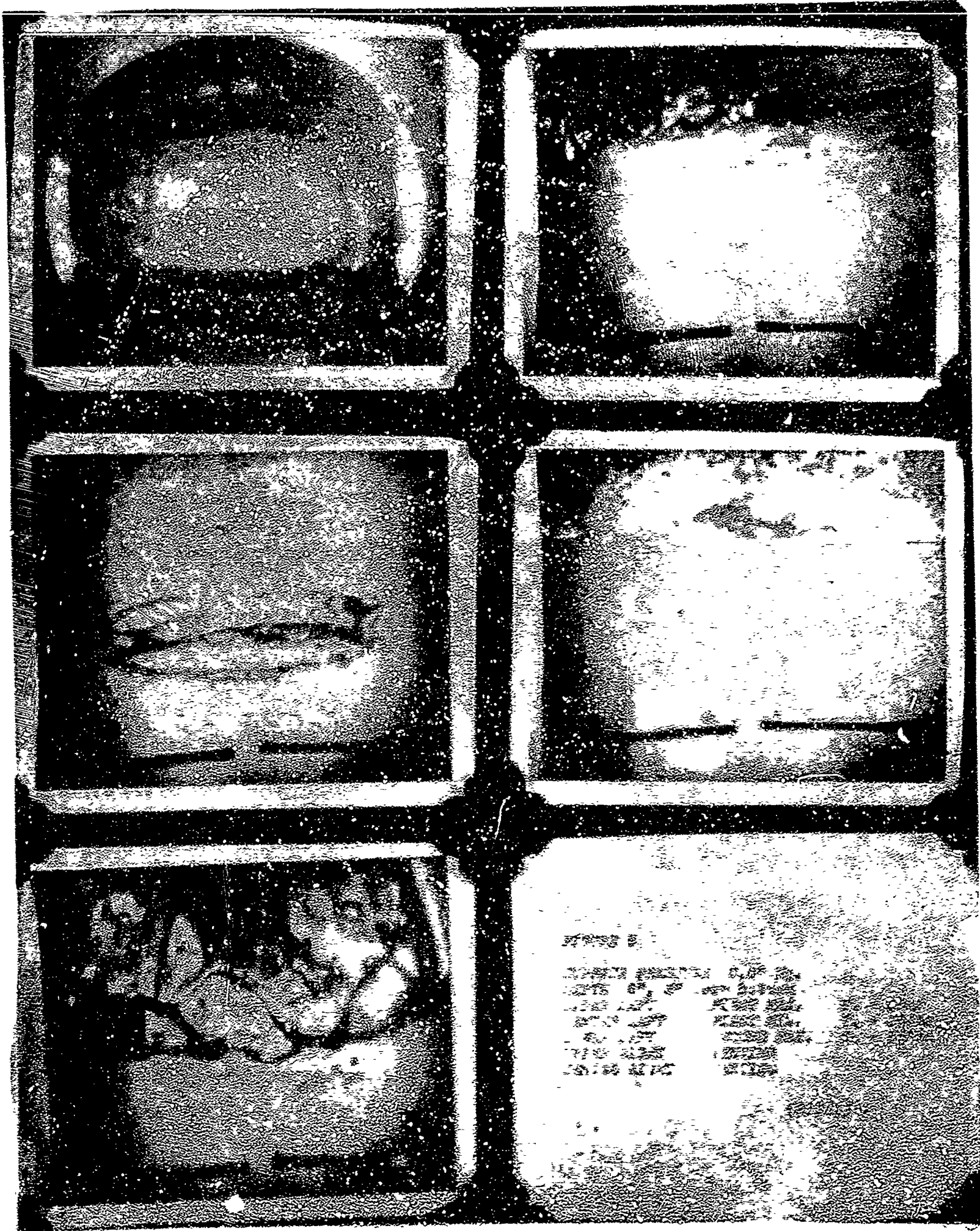
DATE	10/10/68
TIME	10:00
LOCATION	1000 YDS
WEATHER	1000 YDS
WIND	1000 YDS
TEMP	1000 YDS
HUMIDITY	1000 YDS
BAROMETER	1000 YDS
RELATIVE HUMIDITY	1000 YDS
WIND DIRECTION	1000 YDS
WIND SPEED	1000 YDS
WIND FORCE	1000 YDS
WIND TYPE	1000 YDS
WIND DIRECTION	1000 YDS
WIND SPEED	1000 YDS
WIND FORCE	1000 YDS
WIND TYPE	1000 YDS











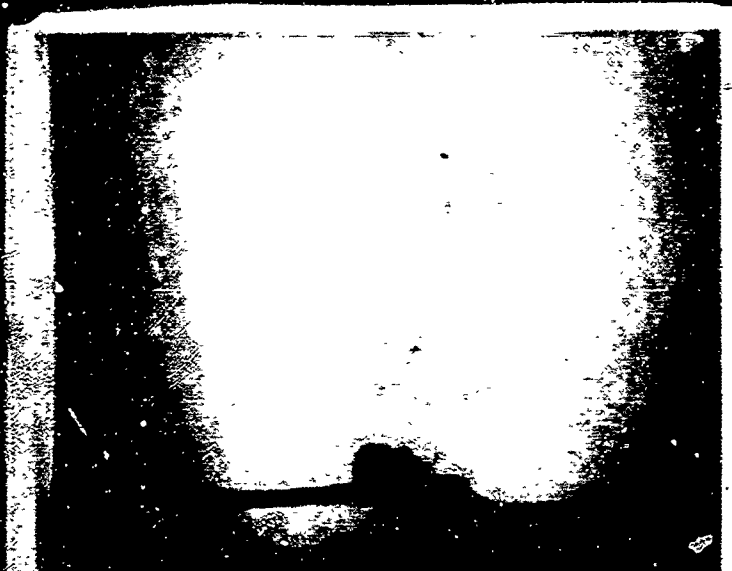
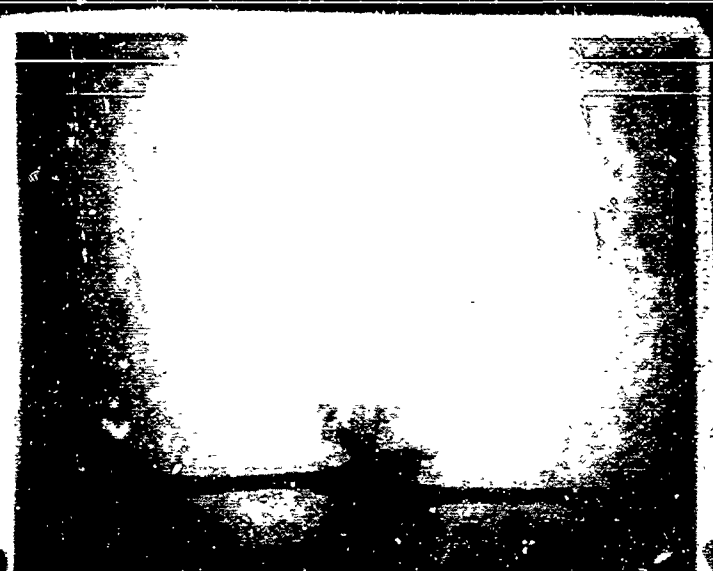
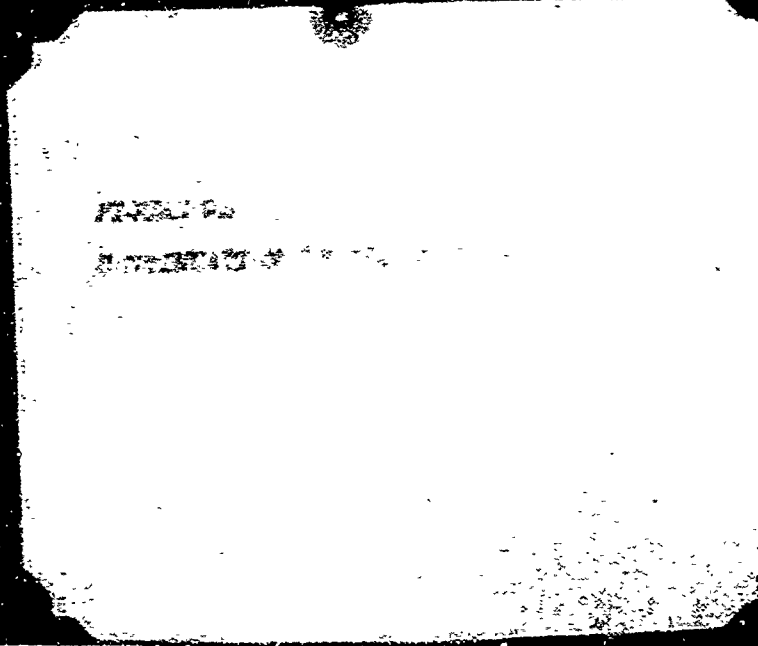
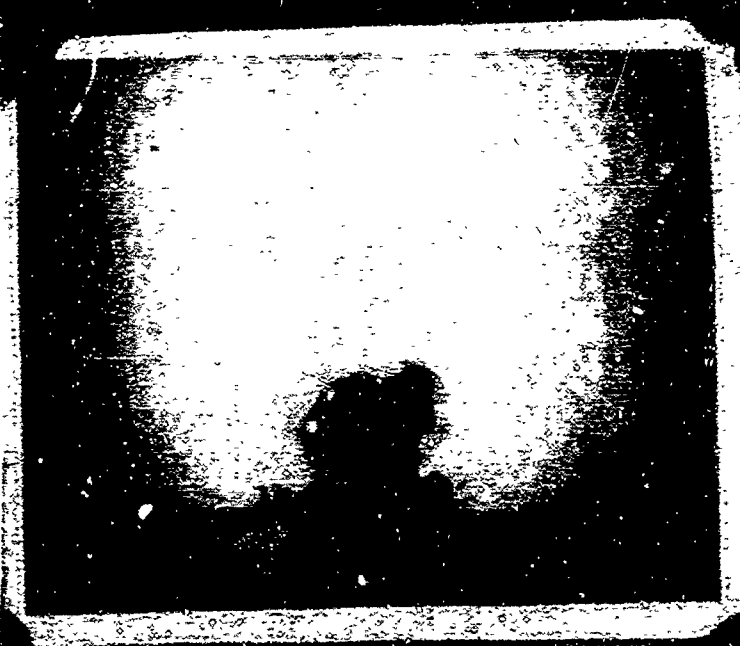
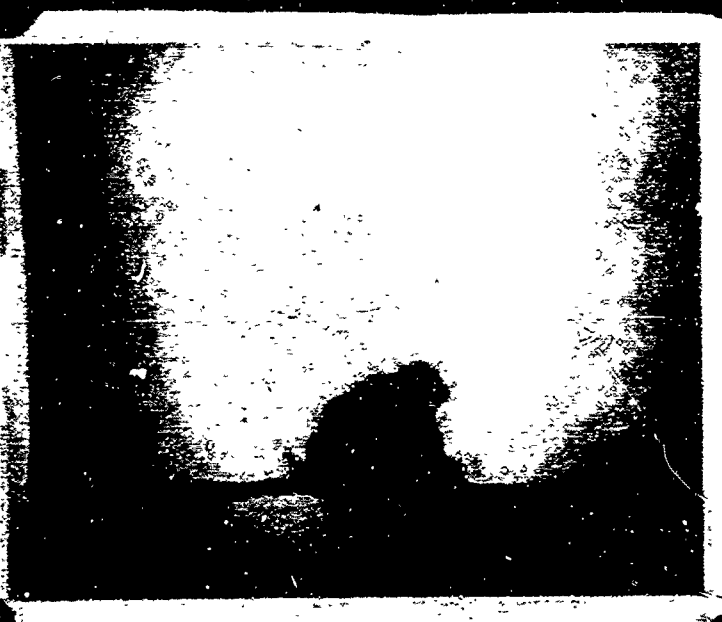
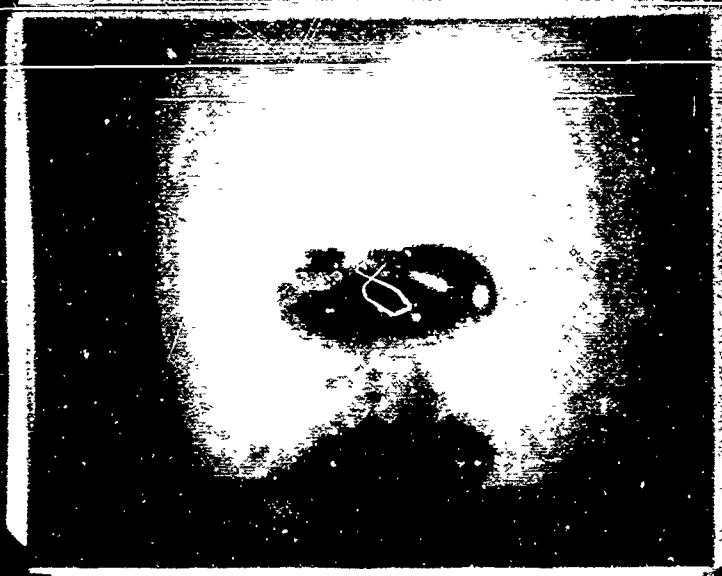
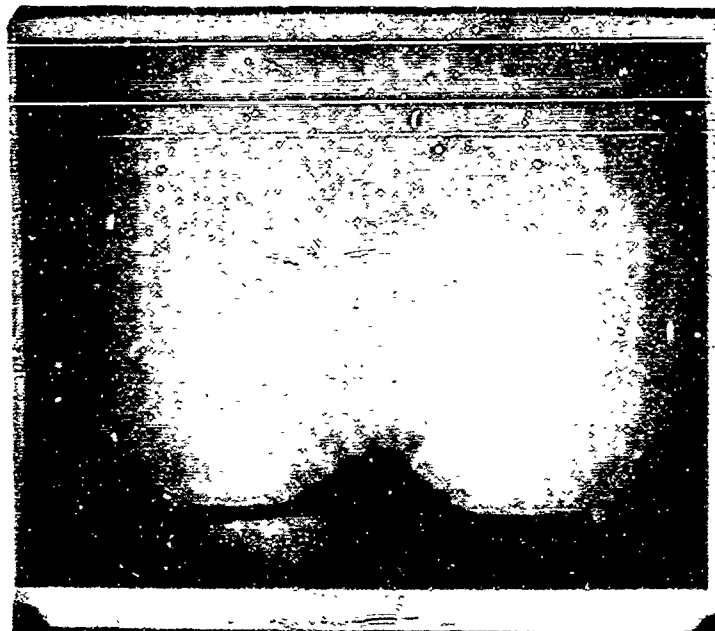


FIGURE 9A

SPACE FREQUENCY 2" sq.		
DEPTH 6", 9" over bottom		
UPPER LEFT	FIRST MAX.	1.5 - 2.0
CENTER LEFT	FIRST MIN.	2.0 - 2.5
LOWER LEFT	SECOND MAX.	2.5 - 3.0
UPPER RIGHT	THIRD MAX.	3.0 - 3.5
CENTER RIGHT	THIRD MIN.	3.5 - 4.0

(11-57)



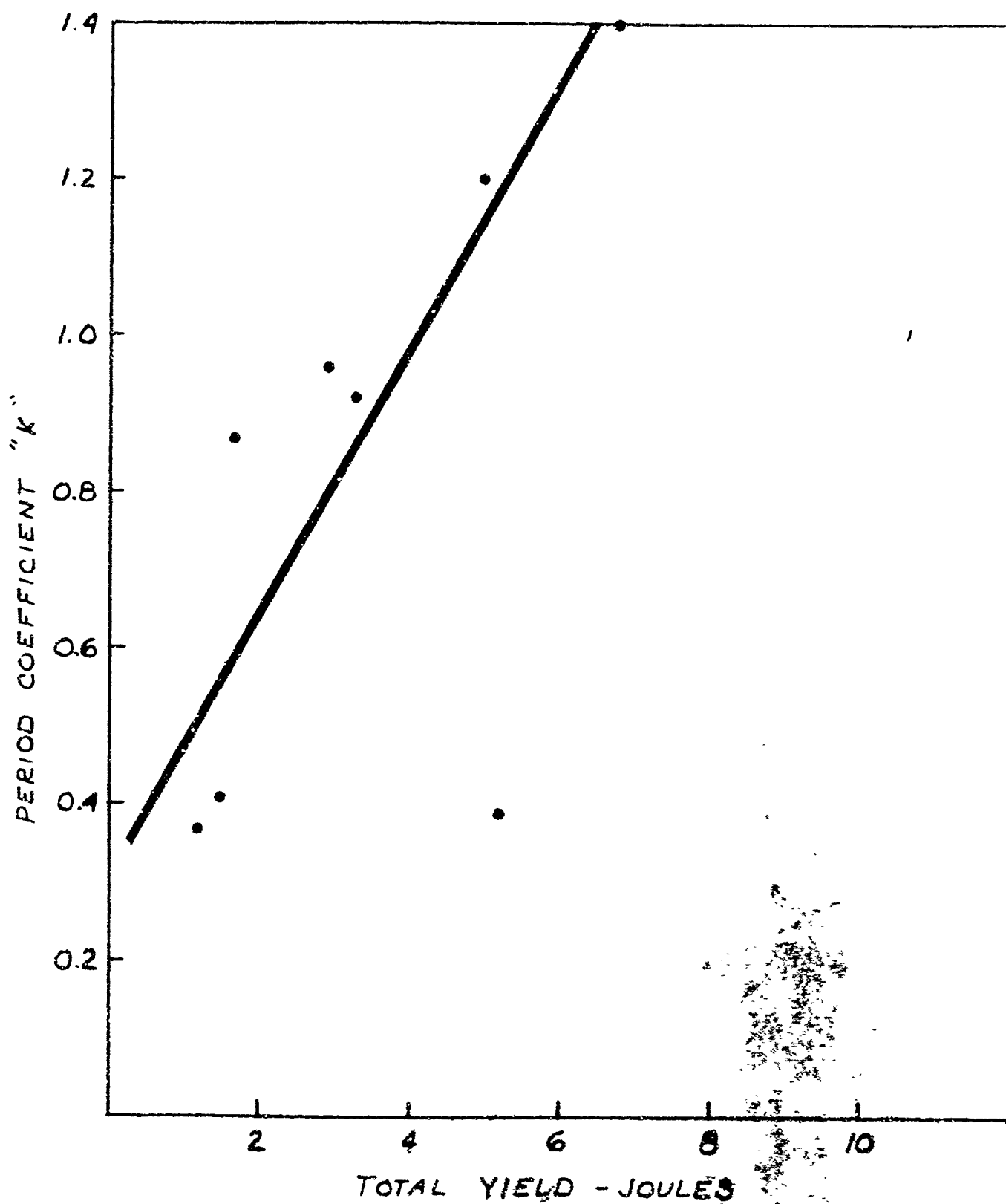


FIGURE 10

FIGURE 11 23

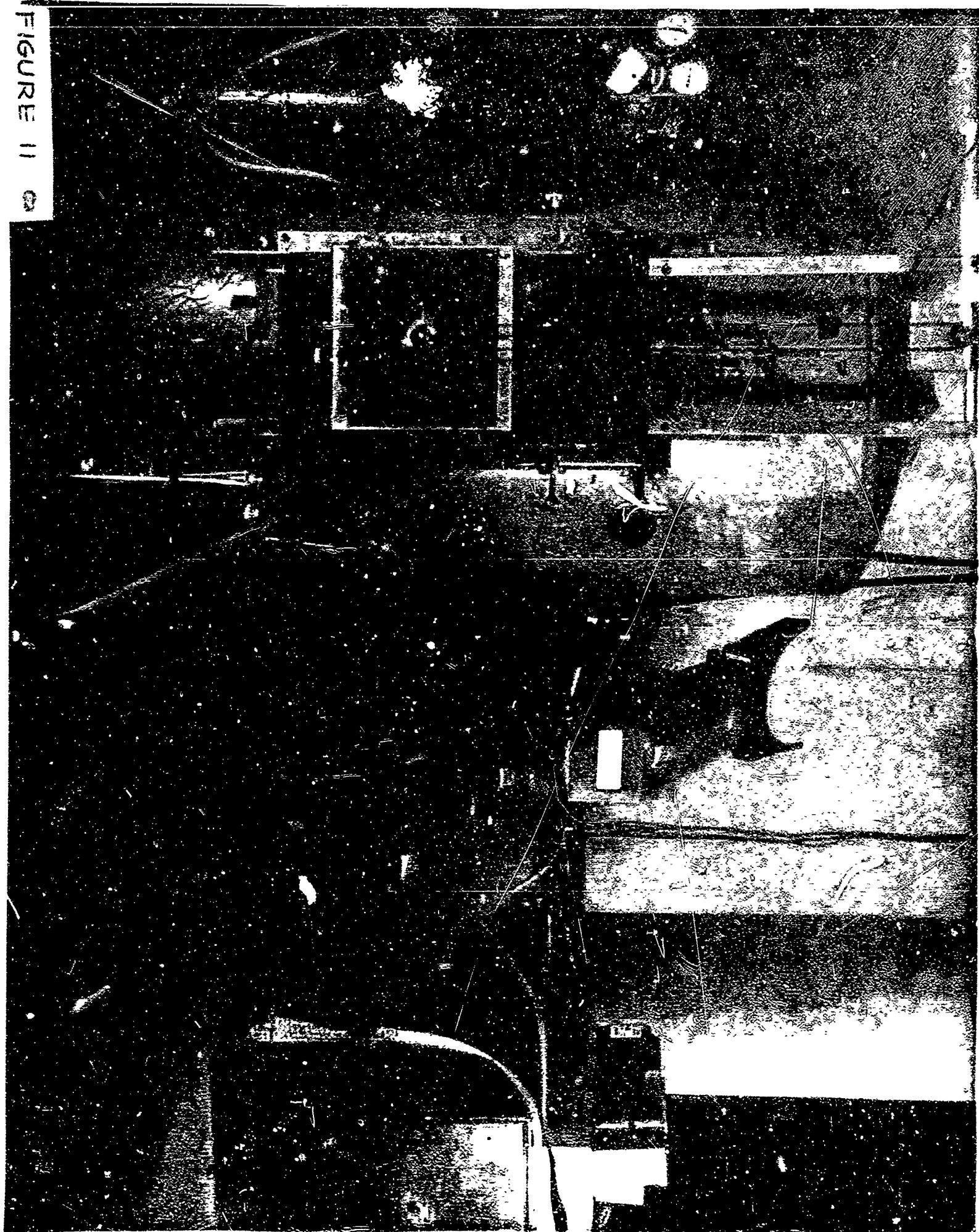




Figure 10

Top - Blue Nile Irrigation
Center - East Nile Irrigation
Bottom - Nile Irrigation



FIGURE 13